Pergamon

PII: S0277-5387(97)00220-9

Polyhedron Vol. 16, No. 22, pp. 3929–3939, 1997

0277-5387/97 $17.00+0.00

Molecular recognition of organic chromophores by coordination polymers: design and construction of nonlinear optical supramolecular assemblies

Songping D. Huang* and Ren-Gen Xiong

Department of Chemistry, University of Puerto Rico, San Juan, PR 00931, Puerto Rico

(Received 30 January 1997; accepted 13 May 1997)

Abstract—One-dimensional coordination polymers of $[Cd(4,4'\text{-bipy})_3(H_2O)_2](ClO_4)_2 \cdot 2H_2O$ (**1**) and $[\{Cd(4,4'\text{-bipy})(H_2O)_2(ClO_4)_2\}(4,4'\text{-bipy})]$ (**2**) were synthesized, respectively, in $EtOH/H_2O$ solution through a self-assembly process or by the ethanothermal reaction in a sealed tube. In the presence of NLO-active organic chromophore 2-nitroaniline or N-methyl-2-nitroaniline, the solution self-assembly reaction gave two-dimensional inclusion compounds of $[\{Cd(4,4'\text{-bipy})_2(H_2O)_2\}(4,4'\text{-bipy})(o\text{-NAN})_2](ClO_4)_2 \cdot H_2O$ where o-NAN = 2-nitroaniline (**3**) and $[\{Cd(4,4'\text{-bipy})_2(ClO_4)_2\}(o\text{-MENAN})_2]$ where o-MENAN = N-methyl-2-nitroaniline (**4**), respectively. The four compounds were characterized by FT-IR, diffuse reflectance UV/VIS, X-ray powder diffraction and single crystal X-ray analysis. © 1997 Elsevier Science Ltd

Keywords: Molecular recognition; nonlinear optical materials; coordination polymers; inclusion compounds; 4,4'-bipyridine; cadmium complexes; X-ray structures; nitroaniline and derivatives.

Design and construction of molecule-based materials exhibiting large second-order nonlinear optical (NLO) responses has and continues to pose a great challenge to synthetic chemists and materials scientists [1–2]. Recently significant advances have been made in incorporating NLO-active organic chromophores into the polymer matrix for electro-optic device applications [3], but rational approaches to designing and synthesizing optimum NLO molecular assemblies are still at a rudimentary level [4]. Besides a host of practical considerations such as optical transparency, processibility and thermal/temporal stability, the most prominent requirements for the second-order NLO effects are [5]: (1) proper alignment of the organic chromophore's dipole moments in the matrix and (2) induction of acentricity to the host-guest system. Strategies employed to achieve these include electric field poling [6], formation of Langmuir–Blodgett films [7], and inclusion in zeolites [8], to just name a few.

We have initiated a research program aimed at using lattice inclusion of organic chromophores inside coordination polymers to achieve optical nonlinearities by a self-assembly approach. Among a plethora of supramolecular assemblies, self-assembled coordination polymers are newer members of the family [9–15]. These novel compounds bridge the gap between molecular and solid state chemistry. In particular, the ordering of organic chromophores into well-defined, infinite one- (1D), two- (2D), and three-dimensional (3D) grids (lattices) formed by the polymer frameworks presents intriguing prospects for the development of novel NLO materials. Compared to the conventional clathration/inclusion method of using discrete molecular hosts such as β-cyclodextrin [16], urea [17], and thiourea [18], our approach offers a unique feature desirable for making NLO materials. For example, further organizing of discrete molecular host–guest assemblies into useful bulk solid materials, whether through crystallization or thin-film formation, often subjects them to dipole moment minimization/cancellation [19]. In contrast, lattice inclusion may *repetitively* place the chromophore guest molecules inside the polymeric frameworks by molecular recognition as such that their dipole moments are aligned without electric field polling.

In this paper, we present the successful synthesis

* Author to whom correspondence should be addressed. Fax: (787)-281-7349.

and structural characterization of four self-assembled metal-organic polymeric compounds, $[Cd(4,4'\text{-bipy})_3(H_2O)_2](ClO_4)_2\cdot 2H_2O$ (**1**) (1D), $[\{Cd(4,4'\text{-bipy})(H_2O)_2(ClO_4)_2\}(4,4'\text{-bipy})]$ (**2**) (1D), $[\{Cd(4,4'\text{-bipy})_2(H_2O)_2\}(4,4'\text{-bipy})(o\text{-NAN})_2](ClO_4)_2\cdot H_2O$ where *o*-NAN = 2-nitroaniline (**3**) (2D) and $[\{Cd(4,4'\text{-bipy})_2(ClO_4)_2\}(o\text{-MENAN})_2]$ where *o*-MENAN = N-methyl-2-nitroaniline (**4**) (2D). We wish to demonstrate the feasibility of using lattice inclusion to construct novel NLO materials as well as the possibility of inducing acentricity to the host–guest system through proper choosing of the guest molecule.

RESULTS AND DISCUSSION

Synthesis and spectroscopic characterization

Compounds **1**, **3** and **4** were prepared in $EtOH/H_2O$ solution through the self-assembly process. Compound **2** was synthesized by the ethanothermal reaction in a sealed Pyrex tube. In either case, pure single-crystal product can be reproducibly obtained in high yield. None of these compounds is found to be soluble in common organic solvents such as THF, acetone, CH_2Cl_2, and CH_3CN or water. To assess phase purity, the products were routinely examined by X-ray powder diffraction. Furthermore, the observed X-ray powder diffraction patterns of the bulk materials were compared with those calculated from the X-ray single-crystal data to ensure that the specimen selected for the X-ray single-crystal structure analysis is representative of the product (see Figs 1–4 of the supporting materials). Because absorption characteristics of the compounds in the UV–vis region is relevant to their nonlinear optical properties, we studied their diffuse reflectance UV–vis spectra. Each compound shows a broad band at ~280 nm which is essentially identical to that of free 4,4'-bipyridine, and in the case of inclusion compound, a broad band of the organic guest chromophore as shown in Fig 1. In addition, the compounds all show IR bands characteristic of the ligands/guest molecules (see Experimental).

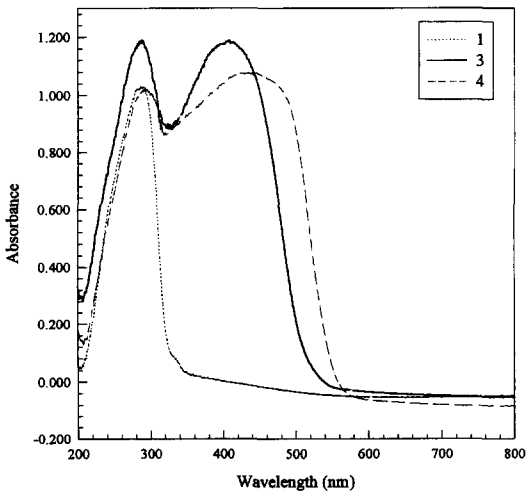

Fig. 1. The diffuse reflectance UV–vis spectra of **1**, **3** and **4**.

Structural description

$[Cd(4,4'\text{-bipy})_3(H_2O)_2](ClO_4)_2\cdot 2H_2O$ (**1**). As a manifestation of its internal symmetry, this compound crystallizes in the orthorhombic space group $P2_12_12$ (#18). The asymmetric unit contains a Cd^{2+} ion, two 4,4'-bipy ligands, a ClO_4^- anion and a crystallization water. The Cd^{2+} ion and one 4,4'-bipy are both situated on the 2-fold rotation axis. Perpendicular to this direction another 4,4'-bipy and the water are bound to the Cd^{2+}. In addition to the 2-fold rotation operation, this unit is then repeated by a cell translation along the *c* edge to generate the one-dimensional chain. Therefore, the Cd···Cd separation within the chain is identical to the length of the *c*-axis (11.674(2) Å). The Cd^{2+} ion can be best described as having *trans* octahedral coordination. Figure 2 depicts the structure of an individual $[Cd(4,4'\text{-bipy})_3(H_2O)_2]_n^{2n+}$ chain. The ClO_4^- is located at the corner defined by the 4,4'-bipy-Cd-4,4'-bipy, slightly touching the van der Waals spheres of two H-atoms each from a 4,4'-bipy ligand as shown in Fig. 3. Because of the interchain Cd···Cd separations of 12.882(3) Å along the b direction, two termina, 4,4'-bipy ligands from the adjacent chains have to stack on top of each other. Figure 4 shows the packing diagram of the unit cell.

$[\{Cd(4,4'\text{-bipy})(H_2O)_2(ClO_4)_2\}(4,4'\text{-bipy})]$ (**2**). Due partly to the presence of the uncoordinate 4,4'-bipy molecules in the lattice, this one-dimensional compound crystallizes in the triclinic space group $P(-1)$ (#2). The asymmetric unit contains a Cd^{2+} ion bound to a 4,4'-bipy ligand, a ClO_4^- group and a H_2O molecule, and a half free 4,4'-bipy unit. The Cd^+ is situated on a center of inversion (1, 1/2, 1), and the free 4,4'-bipy unit is located around another center of inversion (0, 0, 1/2). Both the *trans* octahedral coordination around the Cd^{2+} ion and the full uncoordinate 4,4'-bipy molecule can be generated by inversion operations. Figure 5 shows the unit cell packing diagram of **2**. The N- and H-atom on one side of the 'free' 4,4'-bipy interact, respectively, with coordinate H_2O and ClO_4^- in an alternate fashion between the two adjacent chains. On the whole, the compound may be described as a 1D intercalation complex as shown in Fig. 6.

$[\{Cd(4,4'\text{-bipy})_2(H_2O)_2\}(4,4'\text{-bipy})(o\text{-NAN})_2](ClO_4)_2\cdot H_2O$ (**3**). The compound crystallizes in the C-centered acentric space group $C2$ (#5) with the asymmetric unit containing two Cd^{2+} ions, three coordinate 4,4'-bipy ligands, two ClO_4^- anions, a free 4,4'-bipy, two 2-nitroaniline molecules and a crystallization water. The Cd^{2+} ions, situated, respectively, on the 2-fold rotation axes (1/2, 0.5021, 0) and (1/2, 0.4161, 1/2), are each coordinated by a 4,4'-bipy along the 2-fold axes, and bridged by a common 4,4'-

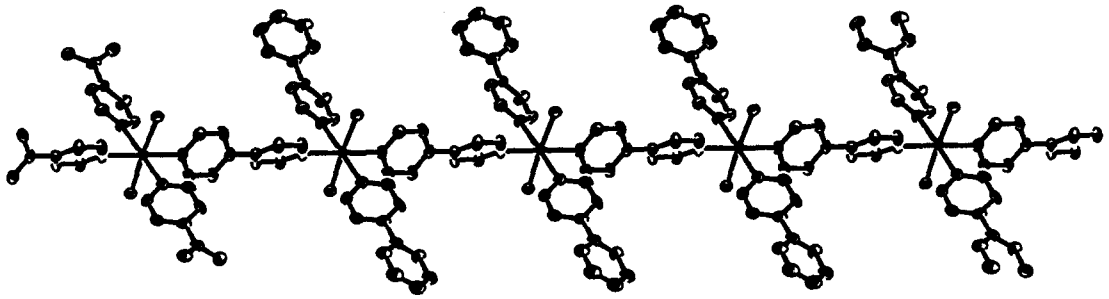

Fig. 2. The structure of an individual $[Cd(4,4'\text{-bipy})_3(H_2O)_2]_n^{2n+}$ chain in **1**.

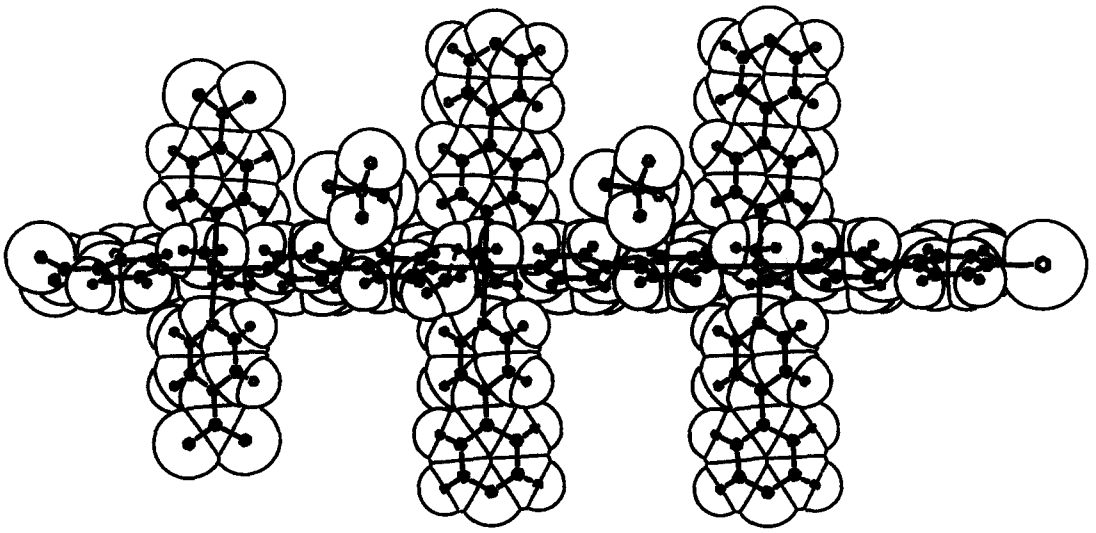

Fig. 3. The interactions of ClO_4^- anions with the $[Cd(4,4'\text{-bipy})_3(H_2O)_2]_n^{2n+}$ chains in **1**.

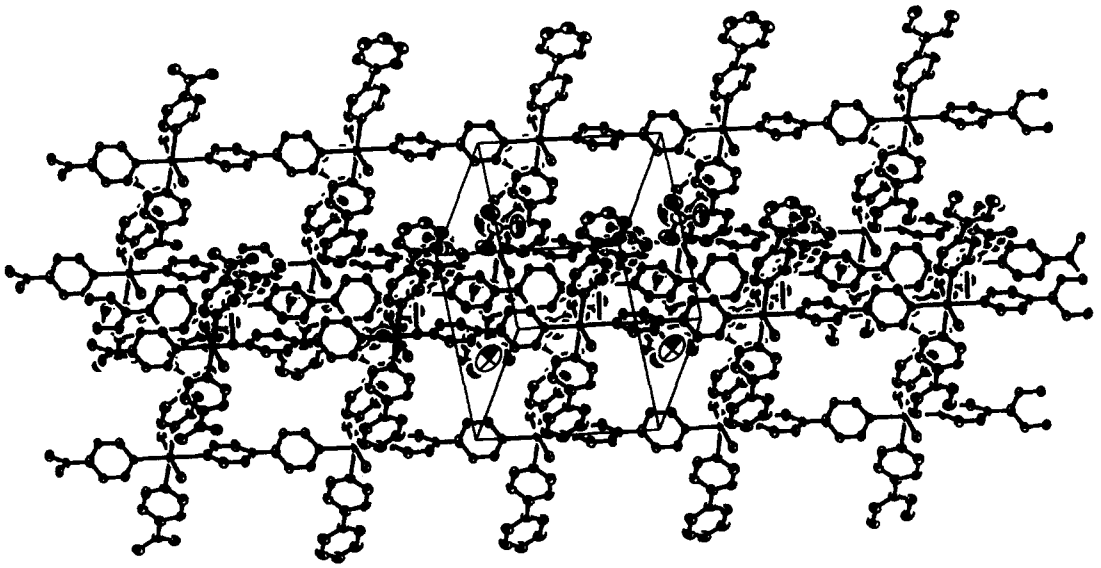

Fig. 4. The unit cell packing diagram for **1**.

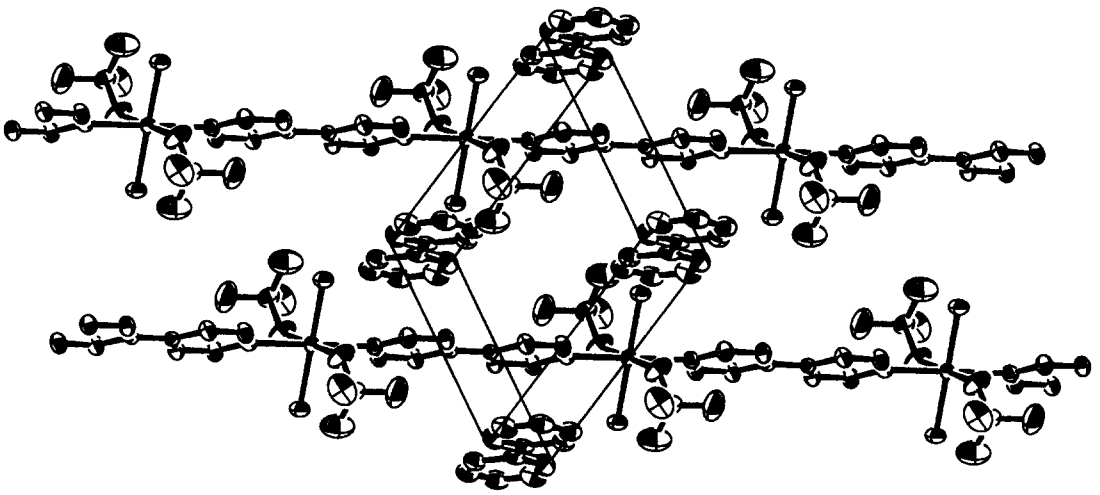

Fig. 5. The unit cell packing diagram for **2**.

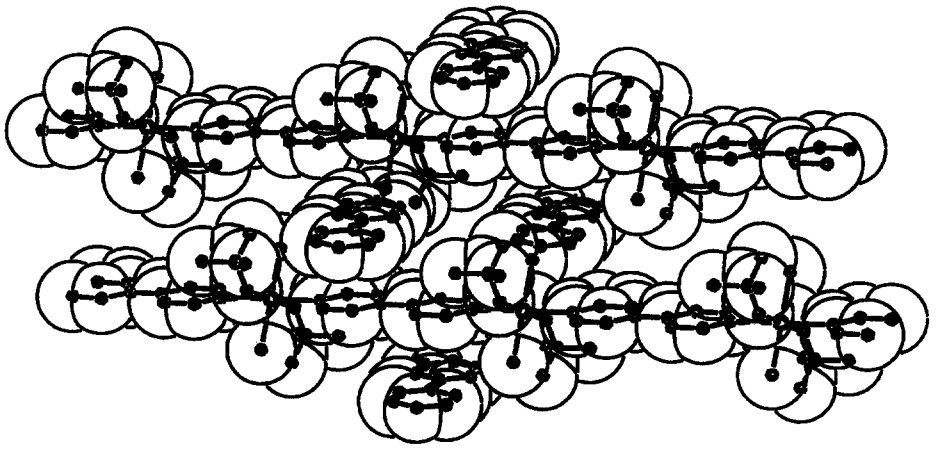

Fig. 6. The interactions of the intercalated 4,4′-bipy ligands with coordinate H_2O and ClO_4^- in **2**.

bipy ligand. The layers are generated by a combination of the 2-fold rotation and unit cell translation in the *b*-direction. The square grids are therefore defined by the Cd···Cd separations of 11.750(3) Å along the *b*-axis and 11.66 Å along the *c*-axis [20]. The layers are separated at about $a/2 = 8.897$ Å. Figure 7 is the ORTEP representation of an individual layer. The two 2-nitroaniline molecules, along with two ClO_4^- anions and a free 4,4′-bipy, are located between the layers. Figure 8 is the packing diagram of **3** while a close-up view of the guest molecules and a ClO_4^- anion is shown in Figure 9. The most conspicuous feature is that the dipole moments of the two different 2-nitroaniline molecules are each oriented with their counterparts below or above the layer to the same direction (see Fig. 8). Such an ordering runs across the entire crystal lattice.

[{Cd(4,4′-bipy)$_2$(ClO$_4$)$_2$}(*o*)-MENAN)$_2$] (**4**). The compound belongs to the centric space group $P2_1/n$ (#14). The asymmetric unit consists of a Cd^{2+} ion, two 4,4′-bipy ligands, a ClO_4^- anion and an N-methyl-2-nitroaniline. The Cd^{2+} ion, bound by two 4,4′-bipy ligands and a ClO_4^- anion, is situated on the center of inversion. The layers are coincided with the (101) plane as shown in Fig. 10. The Cd···Cd separations can be estimated to be 11.74 Å, and the inter-layer distances are 8.72 Å. The N-methyl-2-nitroaniline molecules are resided inside the squares. Each two relate each other by inversion, and are disposed around the metal center so that the methyl H-atoms can interact with the unbound O-atoms of the coordinate ClO_4^- anions.

DISCUSSION

As a control experiment, we first investigated the reaction of Cd^{2+} with 4,4′-bipyridine in the molar ratios of 1 : 1, 1 : 2 and 1 : 3 using ClO_4^- as the counterion. Of particular interest to our inclusion studies were the 2D and 3D polymers, but we were aware that the octahedral geometry of the Cd^{2+} ion combined with bis- and tetra-water coordination should in principle give 1D, 2D and 3D structures. To our surprise,

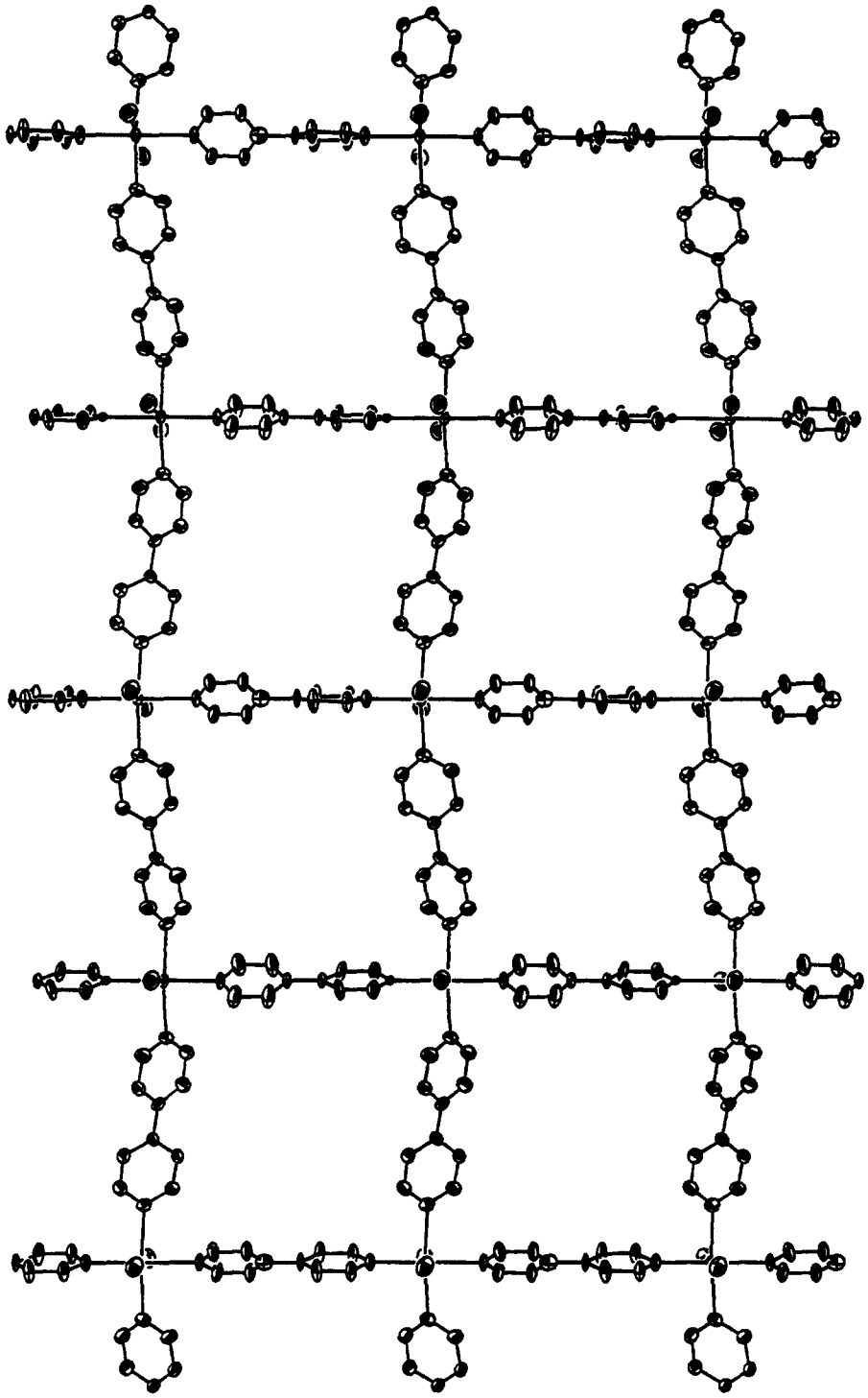

Fig. 7. The ORTEP representation of an individual $[Cd(4,4'\text{-bipy})_2(H_2O)_2]_n^{2+}$ layer in **3**.

all the molar ratios repeatedly afforded $[Cd(4,4'\text{-bipy})_3(H_2O)_2](ClO_4)_2 \cdot 2H_2O$ as the only product. This compound, the first example of a coordination polymer containing terminal 4,4′-bipy ligands, was not expected as opposed to the one-dimensional chains containing tetra-water coordinated Cd^{2+} centers. It seems to be counterintuitive that the structural motif in **1** does not extend to form 2D square grids where the number of interactions per 4-4′-bipyridine would be higher. It is interesting to note that in **1** the ClO_4^- is located near the corner, and interacts with the H-atoms on the 4,4′-bipy. Therefore, we speculate that the formation of the 2D structure with a similar anion packing might increase the enthalpy due to large voids

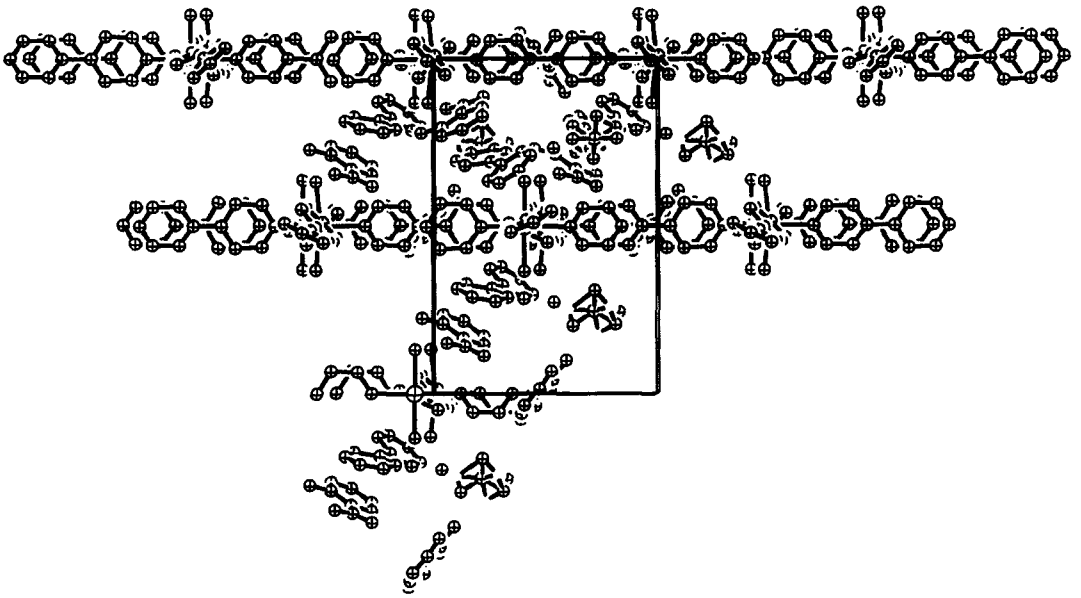

Fig. 8. The unit cell packing diagram for **3**.

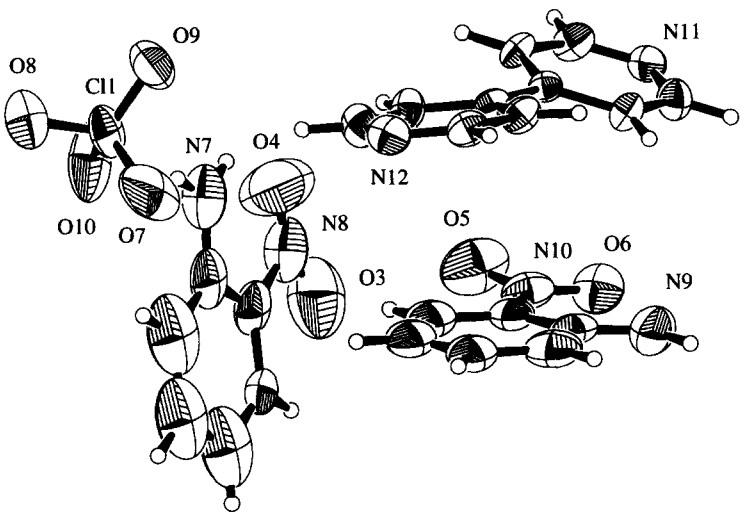

Fig. 9. The orientation of the guest molecules and a ClO_4^- anion in the crystal lattice of **3**.

in the square grids. In order to assess the influence of reaction conditions on structures, we further carried out the reactions with the same molar ratios in superheated ethanol. Again, we obtained another one-dimensional compound [{Cd(4,4′-bipy)$(H_2O)_2$ $(ClO_4)_2$}(4,4′-bipy)] from all three different reaction ratios. This compound contains *trans* coordinate ClO_4^- anions and free 4,4′-bipy molecules. The neutral polymer is structurally similar to a recently reported copper analog [{Cd(4,4′-bipy)$(H_2O)_2(ClO_4)_2$}(4,4′-bipy)] [21]. From these experiments, we conclude that under these conditions, only one-dimensional structures can be formed in the Cd^{2+}/4-4′-bipy/ClO_4^- system [22].

On the other hand, formation of 2D structures can be induced by the presence of a suitable guest molecule. Among a variety of compounds that can act as guests, we are particularly interested in the NLO-active organic chromophores. These are typically π-conjugated molecules with a donor-π-acceptor structure. We chose several simple molecules such as nitroanilines and their derivatives for probing the structure–property relationships. In the case of 2-nitroaniline, the inclusion compound [{Cd(4,4′-bipy)$_2(H_2O)_2$}(4,4′-bipy)(o-NAN)$_2$]$(ClO_4)_2 \cdot H_2O$ crystallizes in a polar space group with the dipole moments of the guest spontaneously aligned. Preliminary experiments by Kurtz powder method showed that **3** is SHG (second-harmonic generation) active. Efforts at measuring and understanding the second-order NLO response for **3** is currently under way. It is worthwhile to point out that 2-nitroaniline,

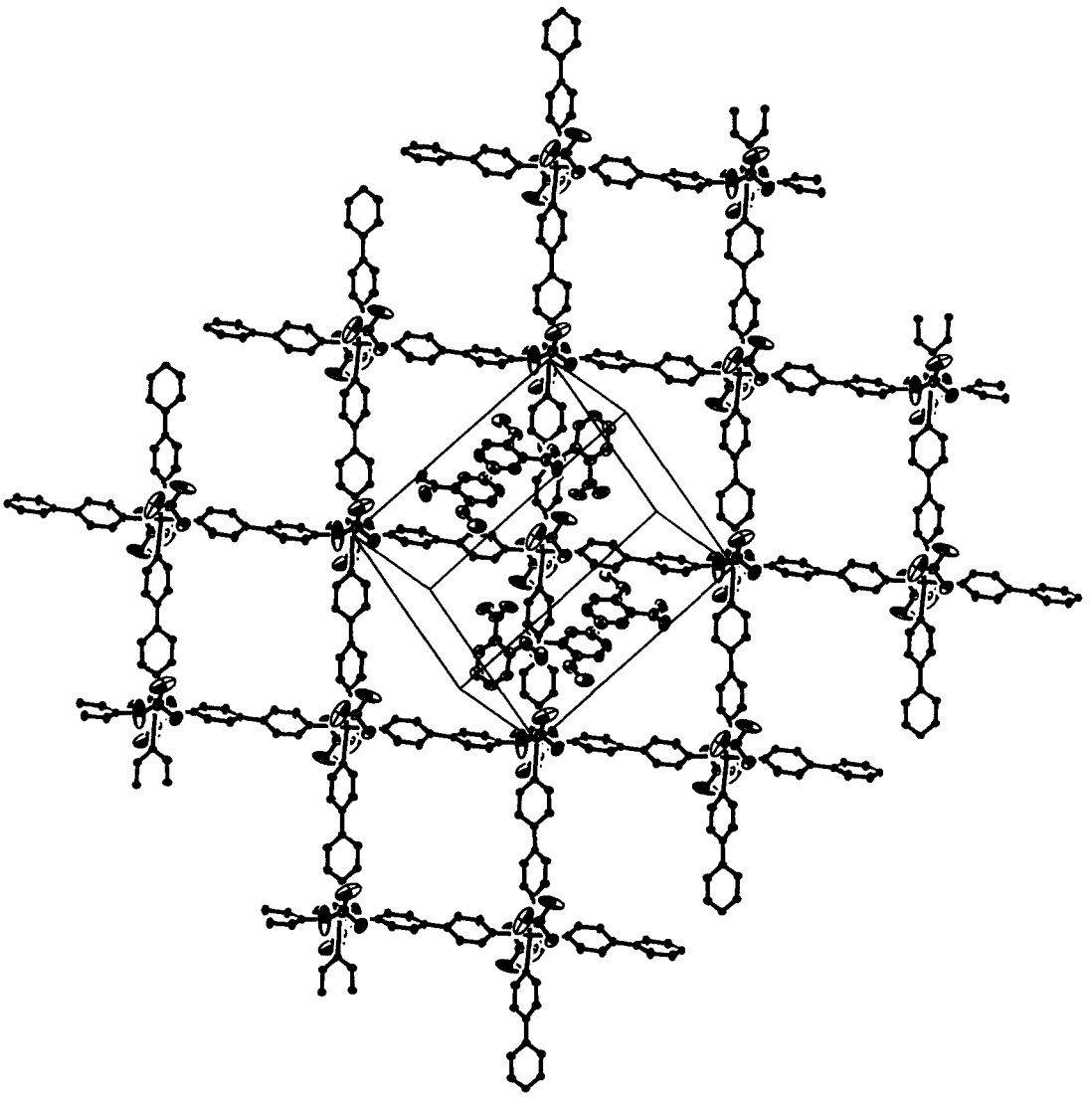

Fig. 10. The unit cell packing diagram for **4**.

a molecule having a large value of molecular first hyperpolarizability β, exhibits no macroscopic second-order NLO effects because the bulk material crystallizes in the centrosymmetric space group $P2_1/a$ (#14). Surprisingly, the N-methyl-2-nitroaniline induces the formation of an entirely different structure, $[\{Cd(4,4'\text{-bipy})_2(ClO_4)_2\}(o\text{-MENAN})_2]$, with a centric crystal packing. In addition, we found that the *meta-* or *para*-nitroaniline cannot induce the formation of any 2D polymeric inclusion compounds [23]. This is consistent with the findings of Fujita and coworkers on the $Cd(NO_3)_2$/4,4'-bipy inclusion studies using *ortho-*, *metal-* and *para*-dihalobenzenes [11(b)]. Thus, the inclusion of guest molecules to the polymers by self-assembly is a subtle molecular recognition process. In other words, the host components do not necessarily view the guest molecules as space-fillers. In contrary, they are keen to respond, by even adjusting the entire assembling mode, to the minor structural change in the guest molecule.

The solution ^1H NMR studies combined with FT-IR and diffuse reflectance UV–vis spectrometry showed that the included guest molecule of 2-nitroaniline or N-methyl-2-nitroaniline can be completely removed by CH_2Cl_2 extraction. We are investigating the possibility of synthesizing ClO_4^- containing 2D host structures, which cannot be prepared directly, by guest-induced self-assembly and subsequent removal of the guest by solvent extraction [24].

CONCLUSION

From this study, the following conclusions may be drawn:

(1) Compared to the methods of intercalation to

layered compounds [25] or inclusion to zeolites, lattice inclusion of organic chromophores in coordination polymer frameworks affords infinite, crystalline compounds with well-defined stoichiometries and structures, thus offering opportunities for probing the structure–property relationship.

(2) Because the self-assembly process can be highly influenced by the presence of different guest molecules, counterions and reaction conditions, it provides a unique tailorbility for making optimum supramolecular assemblies as nonlinear optical materials (e.g. induction of acentricity).

(3) Furthermore, it should be possible to "engineer" other useful, ordered molecular assemblies such as organic radicals/spin-active polymer hosts by a similar approach. New research opportunities abound in this area.

EXPERIMENTAL

Chemicals and solvents in this work were purchased from Aldrich and used as obtained. All manipulations were performed in air. The FT-IR spectra were recorded as solids in KBr matrix in the range of 4000–400 cm^{-1} with the use of a Nicolet 750 FT-IR spectrometer. The diffuse reflectance UV–vis spectra were measured on a Variant Cary 1E spectrophotometer equipped with a 73-mm diameter integrating sphere. Proton NMR experiments were carried out using a GE 300 MHz NMR spectrometer.

Preparation

$[Cd(4,4'\text{-bipy})_3(H_2O)_2](ClO_4)_2 \cdot 2H_2O$ (**1**). To a 20 cm^3 ethanol solution containing $Cd(ClO_4)_2 \cdot 6H_2O$ (311 mg, 1.0 mmol) and 4,4′-bipyridine (468 mg, 3.0 mol) under stirring was added water dropwise until the solution became clear (~3 cm^3 H_2O required). After refluxed for 3 h and cooled to room temperature, the solution was filtered by suction. The filtrate was left to stand at room temperature for one week. After filtration and washing with ethanol and diethyl–ether, colorless single crystals of **1** were obtained in 78% yield. The characteristic IR bands include: aromatic C—C and C—N stretching: 1598(s), 1525(s), 1491(m), 1406(s) cm^{-1}; ClO_4^-: 1080(s, multiple) cm^{-1}.

$[\{Cd(4,4'\text{-bipy})(H_2O)_2(ClO_4)_2\}(4,4'\text{-bipy})]$ (**2**). A sample of 155 mg (0.5 mmol) $Cd(ClO_4)_2 \cdot 6H_2O$ and 156 mg (1.0 mmol) 4,4′-bipyridine was ground and mixed thoroughly in a mortar with a pestle. The reagents were loaded into a thick-walled Pyrex tube (~25 cm long). After addition of 0.4 ml EtOH, the tube was frozen with liquid N_2, evacuated under vacuum and sealed with a flame. The tube was heated at 90°C for 12 h to afford colorless single crystals of **2**. The product was isolated by ethanol and diethyl–ether washing in 93% yield. The characteristic IR bands include: aromatic C—C and C—N stretching: 1592(s), 1530(s), 1491(m) and 1412(s) cm^{-1}; ClO_4^-: 1159–1046(s, extremely broad) cm^{-1}.

$[\{Cd(4,4'\text{-bipy})_2(H_2O)_2\}(4,4'\text{-bipy})(o\text{-NAN})_2](ClO_4)_2 \cdot H_2O$ (**3**). In a typical experiment, water was added dropwise to a 20-ml ethanol solution containing $Cd(ClO_4)_2 \cdot 6H_2O$ (155 mg, 0.5 mmol), 4,4′-bipyridine (156 mg, 1.0 mol) and 2-nitroaniline (284 mg, 2.0 mol) under stirring to clear the solution. After refluxed for 3 h and cooled to room temperature, the solution was filtered. The filtrate was transferred to a 25 cm^3 Erlenmeyer flask, covered with a filtration paper. The solution was left to stand in an air-conditioned room ($T = 22°C$) free of mechanic vibration. Orange rhomb-shaped crystals of **3** with the size up to *ca* 0.9 cm were separated in 4–6 weeks. The crystals were collected, washed with ethanol and diethyl–ether. The isolated yield is 49%. The characteristic IR bands include: NH stretching: 3401(m, sharp) cm^{-1}; aromatic C—C and C—N stretching: 1626(s), 1598(s), 1558(s), 1525(s), 1491(s) and 1412(s) cm^{-1}; NO_2 stretching: 1333(s) and 1243(s) cm^{-1}; ClO_4^-: 1086(s, br and multiple) cm^{-1}.

$[\{Cd(4,4'\text{-bipy})_2(ClO_4)_2\}(o\text{-MENAN})_2]$ (**4**). The pale yellow crystals of **4** were prepared in a similar way as **3** using N-methyl-2-nitroaniline (312 mg, 2.0 mol) in place of 2-nitroaniline. The needle-shaped crystals tend to form large clusters. The estimated yield for **4** is 57%. The characteristic IR bands include: NH stretching: 3392(s, sharp) cm^{-1}; aromatic C—C and C—N stretching: 1603(s), 1598(s), 1570(s), 1536(s), 1502(s) and 1412(s) cm^{-1}; NO_2 stretching: 1322(s) and 1260(s) cm^{-1}; ClO_4^-: 1120(s, br) and 1030 (s, br and multiple) cm^{-1}.

X-ray data collection, structure solution and refinement

All the single crystal X-ray diffraction experiments were carried at room temperature using either an Enraf–Nonius CAD4, a Siemens P4 or a SMART CCD diffractometer equipped with monochromated Mo-Kα radiation ($\lambda = 0.71069$ Å). In each case, a suitable crystal was quickly separated from the mother liquor and coated with epoxy. Unit cell parameters for **1–3** were obtained from a least-squares analysis of 25 reflections in the range of $14 \leqslant \theta \leqslant 16°$. The unit cell parameters for **4** were based upon the least-squares refinement of three dimensional centroids of 6192 reflections. Appropriate cell angles were constrained to their ideal values for **1, 3** and **4**.

Intensity data for **1–3** were collected using a ω–2θ scan mode. The stability of the experimental setup and crystal integrity for each data collection was monitored by measuring three representative reflections at 200 reflection intervals. No decay was detected. The diffracted intensities were collected for Lorentz, polarization and background effects. An empirical absorption correction based upon ψ scans with $\chi \sim 90°$ of three strong reflections was applied to each data set from **1** to **3**. The intensity data for **4**

Table 1. Data for crystal structure analysis of **1–4**

Compound	**1**	**2**	**3**	**4**
Formula	$C_{30}H_{32}CdCl_2N_6O_{12}$	$C_{20}H_{20}CdCl_2N_4O_{10}$	$C_{42}H_{42}CdCl_2N_{10}O_{15}$	$C_{34}H_{32}CdCl_2N_8O_{12}$
a (Å)	13.341(2)	7.590(2)	17.793(4)	8.9175(4)
b (Å)	12.882(3)	9.063(2)	11.750(3)	16.3672(8)
c (Å)	11.674(2)	10.266(2)	23.314(5)	13.1593(6)
α (°)	90.00	106.03(1)	90.00	90.00
β (°)	90.00	95.19(2)	100.68(1)	97.568(1)
γ (°)	90.00	109.01(2)	90.00	90.00
Z; V (Å^3)	2; 2006.3(6)	1; 628.9(3)	4; 4790(2)	2, 1903.9(1)
Space group	$P2_12_12$ (#18)	P-1 (#2)	$C2$ (#5)	$P2_1/n$ (#14)
D_{calc} (g/cm^3)	1.41	1.74	1.54	1.62
μ(Mo-Kα) (mm^{-1})	0.739	1.143	0.645	0.788
Crystal size (mm)	$0.54 \times 0.20 \times 0.11$	$0.54 \times 0.22 \times 0.18$	$0.66 \times 0.56 \times 0.52$	$0.63 \times 0.60 \times 0.45$
$2\theta_{max}$, deg	50	50	55	54
T (°C)	22	22	20	22
No. of unique data, total	3059	2208	6254	4237
No. of data used/σ cutoff	$1794/I_0 > 3\sigma(I_0)$	$2106/I_0 > 3\sigma(I_0)$	$5643/I_0 > 2\sigma(I_0)$	$3109/I_0 > 3\sigma(I_0)$
$T_{min/max}$; abs cor	0.916/1.00 ψ-scans	0.403/1.00; ψ-scans/DIFABS	0.786/1.00; ψ-scans	0.763/1.00; redundant refl.
No. of variables	233	169	606	259
No. of atoms per asym unit (including H)	44	29	79	45
Max/min peaks in Final Diff. Map (e$^-$/Å^3)	1.43/−0.51	1.05/−0.64	0.634/−0.775	0.78/−0.87
Final R/R_w (%) GOF	6.07/7.35; 2.26	4.32/5.44; 2.08	4.55/12.58; 1.06[a]	3.65/5.16; 2.41

[a] Refinement based on F^2 using SHELXL-93.

Table 2. Selected bond distances (Å) and bond angles (deg) for **1–4**

		Compound **1**	
Cd—N(1)	2.383(6)	N(1)—Cd—N(1)*	178.9(3)
Cd—N(3)	2.293(7)	N(1)—Cd—N(3)	89.5(2)
Cd—N(4)	2.333(4)	N(1)—Cd—O(1)	87.1(3)
Cd—O(1)		N(3)—Cd—N(4)	90.5(2)
		O(1)—Cd—O(1)*	175.6(3)
		Compound **2**	
Cd—N(1)	2.273(3)	N(1)—Cd—N(1)*	180.0
Cd—O(1)	2.378(4)	N(1)—Cd—O(1)	89.9(1)
Cd—O(5)	2.264(3)	N(1)—Cd—O(5)	90.1(1)
		O(1)—Cd—O(1)*	180.0
		O(5)—Cd—O(5)*	180.0
		Compound **3**	
Cd(1)—N(1)	2.316(11)	N(1)—Cd(1)—N(2)	180.000(1)
Cd(1)—N(2)	2.390(9)	N(1)—Cd(1)—N(5)	87.4(2)
Cd(1)—N(5)	2.360(5)	N(2)—Cd(1)—N(5)	92.6(2)
Cd(1)—O(1)	2.325(5)	N(5)—Cd(1)—N(5)*	92.3(2)
Cd(2)—N(3)	2.271(10)	N(2)—Cd(1)—O(1)	83.9(2)
Cd(2)—N(4)	2.410(12)	O(1)—Cd(1)—O(1)*	96.1(2)
Cd(2)—N(6)	2.358(5)	N(3)—Cd(2)—N(4)	180.000(4)
		N(3)—Cd(2)—N(6)	92.3(2)
		N(4)—Cd(2)—N(6)	92.6(2)
		N(5)—Cd(1)—N(5)*	87.7(2)
		N(4)—Cd(2)—O(2)	89.8(2)
		O(2)—Cd(2)—O(2)*	90.3(2)
		Compound **4**	
Cd—N(1)	2.347(2)	N(1)—Cd—N(1)*	180.0
Cd—N(2)	2.328(2)	N(1)—Cd—N(2)	94.00(9)
Cd—O(1)	2.364(3)	N(1)—Cd—N(2)*	86.00(9)
		N(2)—Cd—N(2)*	180.0
		N(1)—Cd—O(1)	93.1(1)
		N(1)—Cd—O(1)*	86.9(1)
		O(1)—Cd—O(1)*	180.0

were collected using a narrow frame method with scan widths of 0.3° in ω and exposure times of 20 s/frame. Frames were integrated with Siemens SAINT program. An empirical absorption correction based upon redundant reflections was applied to the data set.

The structures were solved by a combination of direct methods and difference Fourier methods, and refined with full-matrix least squares techniques. The calculations were performed using the teXsan crystallographic software package of Molecular Structure Corporation. All the non-hydrogen atoms were refined anisotropically. The positions of the hydrogen atoms were calculated, but not refined. Table 1 gives crystal data and details for structure analysis for the four compounds. Final atomic coordinates for all structures are given in the supporting information. The selected bond distances and bond angles for **1**–**4** are summarized in Table 2.

Each compound was examined by X-ray powder diffraction for the purpose of phase identification. A Siemens D5000 X-ray powder diffractometer equipped with Cu-Kα radiation ($\lambda = 1.5418$ Å) was employed to record the X-ray powder diffraction patterns. The crystals were ground to fine powder and mounted on a microscope slide. To verify the phase purity and homogeneity of the products, the observed X-ray powder diffraction patterns for the bulk materials were compared with those calculated from the X-ray single-crystal data.

Acknowledgements—This work was supported by the U.S. National Science Foundation and Department of Energy through the EPSCoR Programs (OSR-9452893 and DE-FC02-91ER75674). Additional funds were provided by the University of Puerto Rico through Fondo Institucional Para la Investigación (FIPI). We thank the National Institutes of Health for a grant in support of the purchase of a Siemens CCD SMART diffractometer (3S06GM08102-25S1/M1HREV). We also thank Silvina Fioressi and Pura H. Sotero for measuring the diffuse reflectance UV–vis spectra, and Dr Victor Pantojas for collecting X-ray powder diffraction patterns.

REFERENCES

1. (a) *Polymers for Second-Order Nonlinear Optics* (Ed. G. A. Lindsay and K. D. Singer), ACS Symp. Ser. 601, American Chemical Society, Washington, DC (1995); (b) *Molecular Nonlinear Optics* (Ed. J. Zyss), Academic Press, New York (1994); (c) *Molecular Nonlinear Optics: Materials, Physics and Devices* (Ed. J. Zyss), Academic Press, Boston (1993); (d) G. H. Wagnière, *Linear and Nonlinear Optical Properties of Molecules*, VCH Weinheim/Helvetica Chimica Acta, Basel (1993); (e) N. P. Prasad and D. J. Williams, *Introduction of Nonlinear Optical Effects in Molecules and Polymers*, Wiley, New York (1991); (f) *Materials for Nonlinear Optics: Chemical Perspectives* (Ed. by S. R. Marder, J. E. Sohn and G. D. Stucky). ACS Symp. Ser. 455, American Chemical Society, Washington, DC (1991); (g) *Nonlinear Optical Properties of Organic Molecules and Crystals*, Vols 1, 2 (Ed. D. S. Chemla and J. Zyss). Academic Press, New York (1987); (h) *Nonlinear Optical Properties of Organic and Polymeric Materials* (Ed. D. J. Williams). ACS Symp. Ser. 233, American Chemical Society, Washington, DC (1983).
2. For recent reviews, see (a) Marks, T. J. and Ratner, M. A., *Angew. Chem. Int. Ed. Engl.*, 1995, **34,** 155; (b) Long, N. J., *Angew. Chem. Int. Ed. Engl.*, 1995, **34,** 21; (c) Dalton, L. R., Harper, A. W., Ghosn, R., Steir, W. H., Ziari, M., Fetterman, H., Shi, Y., Mustacich, R. V., Jen, A. K.-Y. and Shea, K. J., *Chem. Mater.*, 1995, **7,** 1060; (d) Benning, R. G., *J. Mater. Chem.*, 1995, **5,** 365. (e) *Optical Nonlinearities in Chemistry* (Ed. D. M. Burland), *Chem. Rev.*, 1994, **94**(1).
3. Devices Based on Electro-optic Polymers Begin to Enter Marketplace, *Chem. & Eng. News*, March 4, 1996, 22 and refs therein.
4. (a) Kanis, D. R., Ratner, M. A. and Marks, T. J., *Chem. Rev.*, 1994, **94,** 195; (b) see ref. [2(a)] and refs therein.
5. (a) Marder, S. R., *"Metal-Containing Materials for Nonlinear Optics"* in *Inorganic Materials* (Ed. by D. W. Bruce and D. O'Hare), p. 136, Wiley, Chichester (1992); (b) see ref. [2(e)].
6. (a) Singer, K. D., Sohn, J. E. and Lalama, S. J., *Appl. Phys. Lett.*, 1986, **49,** 248; (b) Meredith, G. A., Van Dusen, J. G. and Williams, D. J., *Macromolecules*, 1982, **15,** 1385.
7. (a) Ashwell, G. J., Jackson, P. D. and Crossland, W. A., *Nature*, 1994, **368,** 438; (b) Flörsheimer, M., Küpfer, M., Bosshard, C., Looser, H. and Günter, P., *Adv. Mater.*, 1992, **4,** 795.
8. (a) Cox, S. D., Gier, T. E., Stucky, G. D. and Bierlein, J. D., *J. Am. Chem. Soc.*, 1988, **110,** 2986; (b) Girnus, I., Pohl, M.-M., Richter-Mendau, J., Schneider, M., Noack, M., Venzke, D. and Caro, J., *Adv. Mater.*, 1995, **7,** 711.
9. (a) Gable, R. W., Hoskins, B. F. and Robson, R., *J. Chem. Soc., Chem. Commun.*, 1990, 1677; (b) Abrahams, B. F., Hoskins, B. F. and Robson, R., *J. Am. Chem. Soc.*, 1991, **113,** 3603.
10. (a) Abrahams, B. F., Robson, R. and Scarlett, N. V. Y., *Angew. Chem. Int. Ed. Engl.*, 1995, **34,** 1203; (b) Batten, S. R., Hoskins, B. F. and Robson, R., *Angew. Chem. Int. Ed. Engl.*, 1995, **34,** 820; (c) Abrahams, B. F., Hoskins, B. F., Michail, D. M. and Robson, R., *Nature*, 1994, **369,** 27; (d) Abrahams, B. F., Hardie, M. J., Hoskins, B. F., Robson, R. and Sutherland, E. E., *J. Chem. Soc. Chem. Commun.*, 1994, 1049.
11. (a) Fujita, M., Kwon, Y. J., Sasaki, O., Yamaguchi, K. and Ogura, K., *J. Am. Chem. Soc.*, 1995, **117,** 7287; (b) Fujita, M., Kwon, Y. J., Washizu, S. and Ogura, K., *J. Am. Chem. Soc.*, 1994, **116,** 1151.
12. (a) Subramanian, S. and Zaworotko, M. J., *Angew. Chem. Int. Ed. Engl.*, 1995, **34,** 2127; (b) Zaworotko, M. J., *Chem. Soc. Rev.*, 1994, **23,** 284; (c) MacGillivray, L. R., Subramanian, S. and Zaworotko, M. J., *J. Chem. Soc., Chem. Commun.*, 1994, 1325.

13. (a) Carlucci, L., Ciani, G., Proserpio, D. M. and Sironi, A., *J. Am. Chem. Soc.*, 1995, **117,** 4562; (b) Carlucci, L., Ciani, G., Proserpio, D. M. and Sironi, A., *J. Chem. Soc., Chem. Commun.*, 1994, 2755.
14. (a) Yaghi, O. M. and Li, H., *J. Am. Chem. Soc.*, 1995, **117,** 10401; (b) Yaghi, O. M. and Li, G., *Angew. Chem. Int. Ed. Engl.*, 1995, **34,** 207.
15. (a) Venkataraman, D., Gardner, G. B., Lee, S. and Moore, J. S., *J. Am. Chem. Soc.*, 1995, **117,** 11600; (b) Venkataraman, D., Lee, S., Zhang, J. and Moore, J. S., *Nature*, 1994, **371,** 591.
16. Tomaru, S., Zembutsu, S., Kawachi, M. and Kobayashi, M., *J. Chem. Soc., Chem. Commun.*, 1984, 1207.
17. (a) Anderson, A. G., Eaton, D. F., Tam, W. and Wang, Y. (E. I. Du Pont de Nemours), US-4818898 (1989); (b) Eaton, D. F., Anderson, A. G., Tam, W. and Wang, Y., *J. Am. Chem. Soc.*, 1987, **109,** 1886.
18. Davies, J. E. D., Kemula, W., Powell, H. M. and Smith, N. O., *J. Inclusion Phenom. Mol. Recognit. Chem.*, 1983, **1,** 3.
19. It has been estimated that ~75% of all achiral compounds crystallize in centric space groups due to the need of canceling the destabilizing dipole–dipole interactions between the adjacent molecules in the lattice, see (a) Wilson, A. J. C., *Acta Cryst. Sect. A*, 1990, **46,** 742; (b) Wilson, A. J. C., *Acta Cryst. Sect. A*, 1988, **44,** 715; (c) Mighell, A. D., Himes, V. L. and Rodgers, J. R., *Acta Cryst. Sect. A*, 1983, **39,** 742.
20. The two Cd^{2+} centers are slightly displaced from each other. The Cd···Cd distance in the *c*-direction can be calculated from $d = [(\delta)^2 + (c/2)^2]^{1/2} = [(0.5021^{-} 0.4161)^2 + (23.314/2)^2]^{1/2} = 11.66$ Å; δ: displacement of the second Cd^{2+} ion with regard to the first one.
21. Chen, X.-M., Tong, M.-L., Luo, Y.-J. and Chen, Z.-N., *Aust. J. Chem.*, 1996, **49,** 835.
22. However, Cd^{2+}-containing 2D and even 3D polymers can be prepared with different anions: Xiong, R. T., Huang, S. D. and Barnes, C. L., to be submitted.
23. In all such reactions, the crystals formed were identified as **1**.
24. Perazza, M., Xiong, R. T. and Huang, S. D., in preparation.
25. Lacroix, P. G., Clément, R., Nakatani, K., Zyss, J. and Ledoux, I., *Science*, 1994, **263,** 658.